DFBO/95/27

Finite Size Scaling Analysis of Biased Diffusion on Fractals

Giovanni Sartoni[1*] and Attilio L. Stella[2†]

[1] *Dipartimento di Fisica and Sezione INFN, Università di Bologna, I-40126 Bologna Italy*

[2] *INFM–Dipartimento di Fisica and Sezione INFN, Università di Padova, I-35131 Padova Italy*

(May 13, 1996)

Abstract

Diffusion on a T fractal lattice under the influence of topological biasing fields is studied by finite size scaling methods. This allows to avoid proliferation and singularities which would arise in a renormalization group approach on infinite system as a consequence of logarithmic diffusion. Within the scheme, logarithmic diffusion is proved on the basis of an analysis of various temporal scales such as first passage time moments and survival probability characteristic time. This confirms and puts on firmer basis previous renormalization group results. A careful study of the asymptotic occupation probabilities of different kinds of lattice points allows to elucidate the mechanism of trapping into dangling ends, which is responsible of the logarithmic time dependence of average displacement.

Pacs numbers: 64.60.Ak, 05.40.+j, 05.60.+w.
Keywords: logarithmic diffusion, bias, finite size scaling.

* Email: sartoni@bo.infn.it
† Email: stella@bo.infn.it

1 Introduction

A particle diffusing under the influence of a random biasing field can exhibit slow diffusion, with average displacement, R, growing in time, t, as some power of $\ln t$ [1-7]. A remarkable exact demonstration of logarithmic diffusion for a particle hopping on a one-dimensional chain and subject at each site to an independent random bias is due to Sinai [7]. There is also evidence, based upon numerical results, that logarithmic diffusion replaces the anomalous power law one, when particles diffuse on fractal structures, like the incipient infinite cluster of percolation, and are subject to a uniform biasing field [8,9]. In this case, though the field is not random, the complexity of the fractal structure conspires with the former in determining possible localization effects, e.g., by pushing and trapping the moving particle into dangling ends. So far, this phenomenon has been modelized, in most cases, by diffusion along comblike structures with teeth of variable length, where a bias pushes the particle towards the tips [10]. Despite the efforts produced, a comprehensive and satisfactory mathematical description and a general physical understanding of the phenomenon of logarithmic diffusion are still lacking. Present insight is mostly limited to the example of a particle diffusing in 1D and subject to a random bias [11]. The case of diffusion on fractal structures under constant bias, which is our concern here, is more problematic. Comblike models of this latter type of diffusion are again basically one-dimensional, and rather far from the complexity of self-similar structures. The accepted picture of bias induced logarithmic diffusion on a fractal, through the mechanism of trapping into dangling ends, is intuitively appealing but rather vague. So, it is worth to further elucidate and test it, in order to have a more reliable description of such a process.

Recently a study of such trapping mechanism has been accomplished by a dynamical renormalization group (RG) analysis of diffusion on deterministic fractal lattices under the influence of a topological bias [12]. Deterministic self-similar structures, though being a mathematical schematization, retain various fundamental features of real random systems, with the advantage of allowing analytical solutions of random walk processes [13-15]. Furthermore, the RG has demonstrated to be a powerful tool in treating dynamics on self-similar structures [14,15], also in the very peculiar singular conditions implied by logarithmic diffusion [12]. Indeed, one should notice that logarithmic time behaviour implies a singular structure for the RG transformation. A standard dynamical RG yields the time rescaling factor l^z, under length rescaling l, which is consistent with power law anomalous diffusion, $R \sim t^{1/z}$. So, logarithmic diffusion clearly corresponds to the $z \to +\infty$ limit, causing $l^z \to \infty$ as well, and thus a singularity in the RG transformation. As claimed in ref.[12], the control of a singular RG transformation should be the key to extract the correct logarithmic time dependence of R. On the other end, a singular RG transformation can be useful only if the RG is carried out exactly [12]. Such a requirement and the consequent need of handling extremely strong singularities reveals a very hard task, implying, by necessity, some ad hoc simplifications and assumptions in the RG approach [12].

In alternative to RG, finite size scaling (FSS) analysis of non-equilibrium dynamical processes [16] can be exploited for the study of power-law anomalous diffusion. Recently a remarkably efficient and straightforward approach to diffusion on finite self-similar trees and hierarchical combs has been proposed [17]. In this approach, through an exact decimation of the master equations and consequent rescalings, the FSS of first-passage time (FPT) moments and survival probability (SP) can be studied.

A FSS based phenomenological RG study of anomalous diffusion offers several advantages with respect to conventional RG strategies. In particular one does not need to care about proliferation problems in the dynamical equations. Thus, one can legitimately wonder whether a similar approach could be used to confirm and elucidate logarithmic anomalous diffusion on fractal structures of the type considered in ref.[12].

In the present paper we apply the methods of ref.[17] to address diffusion on deterministic T-like finite fractal trees in two dimensions, when a topological bias field is acting. We thus generalize these finite size scaling methods [17] to a system exhibiting singular dynamical scaling. At a first sight, this singular scaling could seem to prevent any effective analysis altogether. To the contrary, we are able to derive the FSS behaviour of FPT moments, SP, first-passage probability (FPP) and probability of being at a certain site at time t (the site occupation probability). All these quantities turn out to be controlled by the same time scale, $t^* \sim e^{\alpha L}$, L being the linear size of the finite lattice. This confirms that, in the infinite system, diffusion is logarithmically localized within a distance $R \sim \ln t$, after a time t, as already conjectured [12]. Furthermore, as discussed below, the existence of a single time scale, t^*, characterizing both the fixed observation-point ensemble (yielding the average over the first passage time at a fixed given site, i.e. the FPT moments) and the fixed observation-time one (concerning the average over the walker displacements at time t, $\langle R(t) \rangle$), supplies concrete support to the intuitive hypothesis that bias induced trapping into dangling ends is directly responsible of logarithmically slow diffusion on self-similar structures.

As a further point of interest, our results show that the presence of a singularity in RG transformations at the fixed point does not prevent the FSS hypothesis to hold in this case. This was not a priori obvious in such a circumstance.

As anticipated above, from a methodological viewpoint, the strategy of studying logarithmic diffusion by FSS allows to avoid some of the difficulties involved in renormalising the infinite model. Since finite size analysis requires to consider the infinite time limit of physical quantities while keeping linear dimensions finite, asymptotic time behaviours are extracted while divergences, induced by the singular time rescaling, still have to develop fully. Hence no ad hoc assumptions are needed to handle strong divergences, as it is the case in infinite systems [12].

This article is organised as follows. In the next section we introduce the model of biased diffusion on

deterministic T fractal, and discuss quantities relevant to the description of the random walk process. In the third section the decimation technique of the finite set of master equations is developed and applied to our model. Phenomenological RG transformations of FPP and SP are then derived and the scalings of FPT and characteristic time are calculated. The methods of section 3 are reconsidered in section 4 and used to extract the long time behaviour of occupation probabilities. Several variants of the model, differing in initial and/or boundary conditions are also examined in section 4, to show that these different conditions do not influence the main dynamical scaling properties. Finally section 5 is devoted to discussion and conclusions.

2 Deterministic fractal model of biased diffusion

Diffusion on random ramified self-similar structures can be fruitfully investigated by the study of random walks on deterministic fractal lattices [13-15]. Often these offer the advantage of being simple enough to allow analytical treatment. For definiteness we will focus on a particular realization of our model, the so-called T fractal (see Fig.2.1), a hierarchical tree in 2D, whose fractal dimension is $\bar{d} = \ln 3/\ln 2$ [18]. On such a lattice at some finite generation order n, a particle diffuses by hopping between nearest neighbour (nn) sites. The probability, $P_i(t)$, for the particle to be at site i at time t, obeys the master equation:

$$P_i(t+\tau) = P_i(t) + \sum_{j \neq i} [W_{ij} P_j(t) - W_{ji} P_i(t)] \quad , \tag{2.1}$$

where the sum on the right hand side runs over nn, j, of site i, and W_{ij} is the probability that a particle hops from j to i in time τ. Here it is assumed that $W_{ij} = W_+$ or W_-, according to whether one goes from site j to i following the bond arrow or not, respectively. Arrows are all pointing in the direction of increasing "chemical" distance from the lattice's leftmost site (site 1 of Fig.2.1). Thus the following consistency relations have to be satisfied: $2W_+ + W_- \leq 1$, $W_\pm \leq 1$. Moreover, we assume $W = W_-/W_+ \leq 1$, so that the bias tends to drive the particle towards longer chemical distance from site 1. This is an example of topological bias field, namely a field having a particular direction in the topological space where the hopping process takes place. This is different from the so called Euclidean bias, which is uniformly directed in the Euclidean space onto which the lattice in embedded [13].

We choose site 1 to be the starting point for particle motion: so, the initial condition of eq.(2.1) is $P_i(0) = \delta_{i,1}$. We also impose the rightmost end-tip site of the lattice, i_s, (e.g. number 4 or number 10 of Fig.2.1a or b, respectively) to be a fully absorbing sink, i.e. a position from which the particle can not hop back to other sites of the T fractal ($W_{ji_s} = 0 \quad \forall j$).

Due to the absorbing site, the SP has an exponential decay whose characteristic time is related to the linear size of the lattice. At generation n, a T fractal has linear size $L = 2^{n+1}$. In standard anomalous diffusion processes, where the average displacement, R, scales as $R \sim t^{1/z}$, the characteristic time, t^*, is expected to scale with L as $t^* \sim L^z$. Relying on previous results for the same model without sink and in

the infinite size limit [12], we expect in the present case a logarithmic localization of motion too, thus a scaling $t^* \sim e^{\alpha L}$, with $\alpha > 0$.

Moreover, since i_s is absorbing, its occupation probability, $P_{i_s}(t)$, coincides exactly with the first-passage probability, $P_{FP}(t)$, at time t for that site. P_{i_s} is also closely related to the survival probability, $S(t)$, namely the probability that the particle has not yet reached the output (sink) site at time t. Indeed,

$$S(t) = 1 - \sum_{k=0}^{m} P_{FP}(k\tau) \quad , (\text{with } t = m\tau). \tag{2.2}$$

Putting $\tau = 1$, and applying the time discrete Laplace transform [14,19],

$$\tilde{P}_i^0(\omega_0) = \sum_{m=0}^{\infty} P_i(m)(1+\omega_0)^{-1-m} \quad , \tag{2.3}$$

to eq.(2.1), we get:

$$\left[\alpha(i,\omega) + \sum_{j\neq i} \frac{W_{ji}}{W_+}\right] \tilde{P}_i(\omega) = \sum_{j\neq i} \frac{W_{ij}}{W_+} \tilde{P}_j(\omega) + \delta_{i,1} \quad , \tag{2.4}$$

where $\omega = \omega_0/W_+$, $\tilde{P}_k^0(\omega_0) = \tilde{P}_k(\omega)/W_+$, and the Kronecker's delta reflects the initial condition $P_i(0) = \delta_{i,1}$. According to eq.(2.1) one should have $\alpha(i,\omega) = \omega \quad \forall i$, in eq.(2.4). However, we already introduce these coefficients in view of the fact that sites with different coordination are inequivalent under lattice decimation and consequent rescaling, as we shall see later. It will turn out that $\alpha(i,\omega) = \alpha_1(\omega),\ \alpha_3(\omega)$ or $\alpha_0(\omega)$, according to whether i has coordination 1, 3 or coincides with site 1, respectively. The only parameters entering eq.(2.4) will thus be $\boldsymbol{\alpha} = (\alpha_0, \alpha_1, \alpha_3)$, and W.

When the sink site i_s is considered, we see immediately that Laplace-transforming $P_{i_s}(m) = P_{FP}(m)$, provides the generating function for the FPP, indeed:

$$(\omega_0+1)\frac{\partial \tilde{P}_{FP}^0(\omega_0)}{\partial \omega_0}\Big|_{\omega_0=0} = -\sum_{m=0}^{\infty}(m+1)P_{FP}(m) = -\langle m\rangle - 1 \quad , \tag{2.5}$$

$\langle m\rangle = \langle t\rangle$ is the average FPT. Higher moments of FPT come from higher derivatives of $\tilde{P}_{FP}^0$. E.g., by deriving $\tilde{P}_{FP}^0$ two times one finds:

$$(\omega_0+1)\frac{\partial}{\partial\omega_0}\left((\omega_0+1)\frac{\partial}{\partial\omega_0}\tilde{P}_{FP}^0(\omega_0)\right)\Big|_{\omega_0=0} = \sum_{m=0}^{\infty}(m+1)(m+1)P_{FP}(m) = \langle m^2\rangle + 2\langle m\rangle + 1 \ . \tag{2.6}$$

Clearly most informations about the diffusion process are contained in $\tilde{P}_i^0(\omega_0)$, or equivalently in $\tilde{P}_i(\omega)$. Thus, the analysis of these quantities will be our main concern below.

3 First-passage time and characteristic time scaling

The first-passage probability for the T fractal with an absorbing point at the right end tip, can be

calculated by successive decimations of the Laplace-transformed master equation. Consider the zeroth-order tree of Fig.2.1a, with site 1 being the input site and site 4 the output one. The explicit form of eq.(2.4) reads:

$$\begin{cases} (\alpha_0(\omega)+1)\tilde{P}_1 = W\tilde{P}_2 + 1 \\ (\alpha_3(\omega)+2+W)\tilde{P}_2 = \tilde{P}_1 + W\tilde{P}_3 \\ (\alpha_1(\omega)+W)\tilde{P}_3 = \tilde{P}_2 \\ \left(\omega + \frac{1}{W_+}\right)\tilde{P}_4 = \tilde{P}_2 \end{cases} . \tag{3.1}$$

Solving this system for $\tilde{P}_4$ yields:

$$\tilde{P}_4(\omega) = \frac{\alpha_1(\omega)+W}{(\omega+\frac{1}{W_+})\left\{(\alpha_0(\omega)+1)\left[(\alpha_3(\omega)+2+W)(\alpha_1(\omega)+W)-W\right]-(\alpha_1(\omega)+W)W\right\}} . \tag{3.2}$$

Furthermore, the Laplace-transformed master equation system for the first order tree of Fig.2.1b is:

$$\begin{cases} (\alpha_0(\omega)+1)\tilde{P}_1 = W\tilde{P}_2 + 1 \\ (\alpha_1(\omega)+W)\tilde{P}_i = \tilde{P}_j \\ (\alpha_3(\omega)+2+W)\tilde{P}_i = \tilde{P}_k + W\sum_{j\neq k}\tilde{P}_j \\ (\alpha_3(\omega)+2+W)\tilde{P}_8 = \tilde{P}_4 + W\tilde{P}_9 \\ \left(\omega + \frac{1}{W_+}\right)\tilde{P}_{10} = \tilde{P}_8 \end{cases} , \tag{3.3}$$

Decimating the last generated sites, namely 2, 3, 5, 6, 8, and 9, and eliminating the respective $\tilde{P}_i$'s from system (3.3), we go back to a lattice which is equivalent to the first order one, after rescaling lengths by a factor 2. After suitable redefinitions and site index reordering, the system for the surviving $\tilde{P}$'s can be reduced to a form analogous to (3.1),

$$\begin{cases} (\alpha_0^{(1)}(\omega)+1)\tilde{P}_1^{(1)} = W^{(1)}\tilde{P}_2^{(1)} + 1 \\ (\alpha_3^{(1)}(\omega)+2+W^{(1)})\tilde{P}_2^{(1)} = \tilde{P}_1^{(1)} + W^{(1)}\tilde{P}_3^{(1)} \\ (\alpha_1^{(1)}(\omega)+W^{(1)})\tilde{P}_3^{(1)} = \tilde{P}_2^{(1)} \\ \left(\omega + \frac{1}{W_+}\right)\tilde{P}_4 = \tilde{P}_2^{(1)} \end{cases} , \tag{3.4}$$

with the following identifications:

$$W^{(1)} = W^2 \tag{3.5a}$$

$$\alpha_0^{(1)}(\omega) = \frac{(\alpha_0(\omega)+1)\left[(\alpha_1(\omega)+W)(\alpha_3(\omega)+2+W)-W\right]}{\alpha_1(\omega)+W} - 1 - W \tag{3.5b}$$

$$\alpha_1^{(1)}(\omega) = (\alpha_1(\omega)+W)(\alpha_3(\omega)+2+W) - 2W - W^2 \tag{3.5c}$$

$$\alpha_3^{(1)}(\omega) = \frac{(\alpha_3(\omega)+2+W)\left[(\alpha_1(\omega)+W)(\alpha_3(\omega)+2+W)-W\right]}{\alpha_1(\omega)+W} - 2 - 3W - W^2 \tag{3.5d}$$

$$\tilde{P}^{(1)}_{i'}(\omega) = \frac{\alpha_1(\omega)+W}{(\alpha_1(\omega)+W)(\alpha_3(\omega)+2+W)-W}\tilde{P}_i \quad , \tag{3.5e}$$

with $i'=1$ if $i=1$, $i'=2$ if $i=4$, and so on. The apex (1) in front of all left hand quantities indicates that they have been rescaled once after a decimation. A few remarks about these RG transformations: in first place, quantities relative to the sink site do not rescale, as it appears from the last of eqs.(3.4). In addition one should notice that different $\alpha_i^{(1)}$'s undergo different transformations, the dependence on the original α_i's being nonlinear. This is a standard memory effect associated with dynamical coarse graining. Now the necessity of introducing different α-coefficients becomes clear.

Starting with an nth-order lattice, we perform n successive decimations and rescalings in such a way to arrive to the zeroth-order system. Then, solving the latter for $\tilde{P}_4$, the FPP generating function, we find:

$$\tilde{P}_{FP}(\omega) = \frac{\alpha_1^{(n)}(\omega)+W^{(n)}}{\left(\omega+\frac{1}{W_+}\right)\Delta^{(n)}} \tag{3.6}$$

$$\Delta^{(n)} = (\alpha_0^{(n)}(\omega)+1)\left[(\alpha_3^{(n)}(\omega)+2+W^{(n)})(\alpha_1^{(n)}(\omega)+W^{(n)})-W^{(n)}\right]-W^{(n)}(\alpha_1^{(n)}(\omega)+W^{(n)}) \ .$$

Moments of the first passage time are obtained by the series expansion of $\tilde{P}_{FP}$. Indeed assuming that $\tilde{P}_{FP}$ is expandable around $\omega=0$ (which is justified for a finite system) i.e.

$$\tilde{P}_{FP}(\omega) = p_0 + p_1\omega + p_2\omega^2 + O(\omega^3) \quad , \tag{3.7}$$

we see immediately from (2.5-6) that $p_1 = -\langle t\rangle - 1$ and $p_2 = \langle t^2\rangle + 2\langle t\rangle + 1$ (notice that, since $\frac{\partial \tilde{P}^0_{FP}(\omega_0)}{\partial\omega_0} = \frac{1}{W_+}\frac{\partial \tilde{P}_{FP}(\omega_0/W_+)}{\partial\omega_0} = \frac{\partial \tilde{P}_{FP}(\omega)}{\partial\omega}$, p_i are related to FPT moments without any further rescaling). Thus, once the relation between the p_i's of two successive T Fractal orders is known, one can derive the scaling of $\langle t\rangle$. Since we are interested only in the average FPT we focus on p_1 rescaling. To this aim we have to expand the right hand side of (3.6) and inherent quantities up to first order in ω about $\omega=0$.

To calculate $\boldsymbol{\alpha}^{(n)}(\omega)$ we first consider its series expansion in powers of ω about $\omega=0$. Writing $\alpha_i^{(n)}(\omega) = \sum_k^{\infty}\alpha_i^{(n),k}\omega^k$, and considering (3.5b-d), we are able to derive the relation between $\boldsymbol{\alpha}^{(n),1}$ and $\boldsymbol{\alpha}^{(n-1),1}$, which are needed to calculate the scaling of p_1. By keeping everywhere only leading order in $1/W^{(n)}$ ($W^{(n)} = W^{2^n} = W^{L/2}$), in the explicit relations, we get:

$$\begin{cases} \alpha_0^{(n),1} \cong \dfrac{(1+W)\alpha_1^{(n-1),1}}{W^{(n-1)}} \cong \dfrac{(1+W)2^{n-1}}{W^{2^{n-1}}} \\ \alpha_1^{(n),1} \cong (1+W)2\alpha_1^{(n-1),1} \cong (1+W)2^n \\ \alpha_3^{(n),1} \cong \dfrac{(1+W)2\alpha_1^{(n-1),1}}{W^{(n-1)}} \cong \dfrac{(1+W)2^n}{W^{2^{n-1}}} \end{cases} \ . \tag{3.8}$$

Disregarded terms in (3.8) are $o(W^{2^{n-2}})$, which is negligible for $n \gg 1$, since $W<1$ in the biased case. Expanding (3.6) consistently with the approximation leading to (3.8) then yields:

$$\tilde{P}_{FP}(\omega) \cong \frac{W_+}{W^{(n)}}\left[W^{(n)} - \omega\alpha_1^{(n),1} + O(\omega^2)\right] \quad . \tag{3.9}$$

So $\langle t \rangle$ scales as

$$\langle t \rangle^{(n)} + 1 \cong \frac{2}{W^{(n-1)}} \left(\langle t \rangle^{(n-1)} + 1 \right) \quad , \tag{3.10}$$

and finally we have:

$$\langle t \rangle^{(n)} \sim \frac{2^n}{W^{2^n}} = \frac{L}{2W^{L/2}} = \frac{L}{2} e^{|\ln W| L/2} \quad . \tag{3.11}$$

The survival probability, $S(m)$, defined in (2.2) decays exponentially in m as $S(m) \propto \exp(-m/t_n^*)$, at long times, for any finite nth-order T fractal, due to the absorbing boundary conditions. So, we want to investigate the relation between the characteristic time, t_n^*, and the FPT. $P_{FP}(m)$ decays also exponentially, because it is just the discrete derivative of $S(m)$: $P_{FP}(m) \overset{m \to +\infty}{\propto} \left(e^{1/t_n^*} - 1 \right) e^{-m/t_n^*}$. This implies that $\tilde{P}_{FP}(\omega)$ has a simple pole in $\omega_c = \frac{1}{W_+} \left(e^{-1/t_n^*} - 1 \right)$ in the limit $\omega \to 0$, which corresponds to the long time behaviour of $P_{FP}(m)$.

The characteristic time grows with the T fractal size n, $t_n^* \overset{n \to +\infty}{\longrightarrow} +\infty$; hence $\omega_c \overset{n \to +\infty}{\longrightarrow} 0^-$ and can be located by looking for the simple pole of $\tilde{P}_{FP}$ in the limit $\omega \to 0$ [20]. Expanding numerator and denominator up to order ω on the r.h.s of (3.6), and exploiting (3.8) for the expansion of $\boldsymbol{\alpha}^{(n)}(\omega)$, we eventually arrive to:

$$\tilde{P}_{FP}(\omega) \simeq \frac{\alpha_1^{(n),1} \omega + W^{(n)}}{\left(\omega + \frac{1}{W_+} \right) \left(\omega + \frac{(1+W) W^{(n)}}{2\alpha_1^{(n),1}} \right)} \quad . \tag{3.12}$$

The first simple pole $\omega_c = -\frac{1}{W_+}$ is not related to long time behaviour, since $-\frac{1}{W_+} \leq -1$. The second simple pole is $\omega_c \simeq -\frac{W^{(n)}}{2\alpha_1^{(n),1}} \simeq -\frac{W^{2^n}}{2(1+W)2^n} = -\frac{W^{L/2}}{(1+W)L}$. Since $\omega_c \overset{n \to +\infty}{\cong} \frac{-1}{W_+ t_n^*}$, then

$$t_n^* \sim \frac{2^{n+1}}{W^{2^n}} \sim \frac{L}{W^{L/2}} \quad . \tag{3.13}$$

So diffusion has a characteristic time scale growing exponentially with the system size, and the dynamical exponent, z, diverges as expected. Moreover t_n^* scales like $\langle t \rangle^{(n)}$, and, consistently with infinite lattice result for the average displacement [12], the typical distance, L, travelled in time t is $L \sim \ln t$.

All the above results provide evidence that dynamics is controlled by a single time scale determined by the trapping mechanism into dangling ends. In truly infinite fractal structures [12] dangling ends of all length scales exist, thus dynamics is logarithmically localized.

The existence of a single characteristic time suggests also that fixed time and fixed point of observation ensembles are substantially equivalent in this model, in accordance to what happens in most models of power-law anomalous diffusion on self-similar lattices [13-17].

Finally, two important remarks concerning the approximate calculations are in order. In first place, due to approximation to $o(W^{2^{n-2}})$ introduced to obtain eqs.(3.8) and consequently (3.9) and (3.12), results concerning $\langle t \rangle$ and t^* can not be extended to the region $W \lesssim 1$, of cross-over to the standard anomalous diffusion regime corresponding to $W = 1$ [12,14]. Secondly, we assumed $\tilde{P}_{FP}(\omega)$ to be expandable about

$\omega = 0$ to get (3.9), while we have then seen it has a pole $\omega_c \overset{n\to+\infty}{\longrightarrow} 0^-$. However, since ω_c is finite for any finite n, no matter how large, this will cause no inconsistency, because for ω close enough to 0, an expansion will always be allowed. On the other end, this feature implies that the limits $t \to +\infty$ and $n \to +\infty$ (i.e. $L \to \infty$) can not commute, because when $L \to \infty$ a singularity of $\tilde{P}_{FP}$ sets exactly at $\omega = 0$, thus results (3.9-11) do not extend to that limit. This problem does not exist in principle for the asymptotic analysis of FPP: indeed, the derivation of (3.12,13) involves no analyticity assumption for $\tilde{P}_{FP}$. However, the determination of the $n \to +\infty$ limit remains a serious task in its own due to the presence of strongly divergent $1/W^{2^n}$ terms in RG equations [12].

4 Long time behaviour of the occupation probabilities and trapping mechanism

The knowledge of the occupation probability, $P_j(t)$, of a generic site j of the T fractal at its nth-order, at time t, supplies further information about the dynamics. $P_j(t)$ is also expected to decay exponentially at long times, and we are interested in its characteristic time, which should scale like t^*. Furthermore, since sites with different coordination are dynamically inequivalent (look at different α_i's rescalings in (3.5b-d)), such a feature should extend, in some way, to their occupation probabilities. When these show an asymptotic exponential decay, they should also have an amplitude factor dependent on site coordination and position, and on the bias parameter W as well. The nature of such dependence may provide further insight into the diffusion mechanism.

Asymptotic analysis applied to $P_{FP}(t)$ can be extended, with moderate additional effort, to get also the asymptotics of a generic $P_i(t)$.

Consider again the nth-order T fractal with initial condition at site 1 and absorbing boundary condition at the rightmost end-tip site. We perform n successive decimations of the master equations (2.4), eventually arriving to a system, like (3.4), for the surviving $\tilde{P}^{(n)}$'s, rescaled $n-$times according to (3.5). Now the system can be completely solved for the occupation probabilities of surviving sites, yielding:

$$\tilde{P}_3^{(n)}(\omega) = \frac{1}{\Delta^{(n)}} \tag{4.1a}$$

$$\tilde{P}_1^{(n)}(\omega) = \frac{\left(\alpha_1^{(n)}(\omega) + W^{(n)}\right)\left(\alpha_3^{(n)}(\omega) + 2 + W^{(n)}\right) - W^{(n)}}{\Delta^{(n)}} \tag{4.1b}$$

$$\tilde{P}_2^{(n)}(\omega) = \frac{\alpha_1^{(n)}(\omega) + W^{(n)}}{\Delta^{(n)}} \tag{4.1c}$$

$$\Delta^{(n)} = (\alpha_0^{(n)}(\omega) + 1)\left[(\alpha_1^{(n)}(\omega) + W^{(n)})(\alpha_3^{(n)}(\omega) + 2 + W^{(n)}) - W^{(n)}\right] - W^{(n)}(\alpha_1^{(n)}(\omega) + W^{(n)}) \ ,$$

and $\tilde{P}_4(\omega)$ as in eq.(3.6). Using (3.5e), we then recover the original, unrescaled, $\tilde{P}$'s as:

$$\tilde{P}_i(\omega) = \prod_{k=0}^{n-1}\left[\frac{(\alpha_1^{(k)}(\omega) + W^{(k)})(\alpha_3^{(k)}(\omega) + 2 + W^{(k)}) - W^{(k)}}{\alpha_1^{(k)}(\omega) + W^{(k)}}\right]\tilde{P}_{i'}^{(n)}(\omega) \ , \tag{4.2}$$

where i' is the index that site i takes after n decimations. Again $\tilde{P}(\omega)$ is a fraction and, being concerned with long time behaviours, we expand both numerator and denominator to leading order in ω. In this way we expect to find the single pole corresponding to the characteristic time, like already seen for $\tilde{P}_{FP}(\omega)$. As additional task here, the product preceding $\tilde{P}^{(n)}$ on the r.h.s. of (4.2), has to be expanded. To leading order in ω, this can be accomplished using the series expansions of $\boldsymbol{\alpha}^{(k)}(\omega)$ about $\omega = 0$ and exploiting equations (3.8) for the coefficients $\alpha_i^{(k),1}$. Relations (3.8) are drawn within an accuracy of $o(W^{2^{n-2}})$, which thus applies also to the results below. We shall omit the details of such cumbersome calculations, and give directly the asymptotic expression of occupation probabilities:

$$P_1(t) \approx \frac{\left(1 - W^{2^n}\right)}{1 - W^2} \frac{W^{2^{n+1}}}{4\ 2^n} e^{-t/t_n^*} \tag{4.3a}$$

$$P_4(t) \approx \frac{\left(1 - W^{2^n}\right)}{1 - W^2} \frac{W^{2^n}}{4\ 2^n} e^{-t/t_n^*} \tag{4.3b}$$

$$P_7(t) \approx \frac{\left(1 - W^{2^n}\right)}{1 - W^2} \frac{1}{2\ 2^n} e^{-t/t_n^*} \tag{4.3c}$$

$$P_{10}(t) \approx \frac{W_+}{4(1+W)} \frac{W^{2^n}}{2^n} e^{-t/t_n^*} \tag{4.3d}$$

$$t_n^* \simeq \frac{(1+W)}{W_+} \frac{2^{n+1}}{W^{2^n}} \quad .$$

For purposes which will be clear later on, sites have been labelled with the indexes they have after $n-1$ decimations, consistently with Fig.2.1b. So 1 is the injection site, 10 is the absorbing one, 7 is at the tip of the central branch and 4 is at the lattice center (they correspond to sites 1,4,3,2 of Fig.2.1a, respectively). Note that the characteristic time, t_n^*, is the same we found in (3.13), for every site, while the amplitude dependence on W is rather varying from site to site.

In order to have further terms of comparison it is worth deriving the asymptotic $P(t)$ form for a few other sites too, namely those which disappear due to the nth decimation, but have different chemical distances from both origin and sink. For definiteness we focus on sites 3,6 and 9 which are tips, and on 8 which has three nn (indexes refer always to Fig.2.1b). We suppose to arrest decimation at the $(n-1)$th stage, obtaining a lattice configuration like Fig.2.1b. The site occupation probabilities to be calculated can be drawn by solving the corresponding $(n-1)-$times decimated master equation set for $\tilde{P}_i^{(n-1)}(\omega)$, and using also results (4.1a-c). For example, site 6 is at the same chemical distance from 1 as 7, then 6 and 7 are completely equivalent and their $P(t)$'s show identical long t behaviour. On the other end , site 9, though equally far from the origin as 7, is influenced by the absorbing boundary condition on the branch it belongs to and exhibits different features. Indeed:

$$\tilde{P}_9^{(n-1)}(\omega) = \frac{\tilde{P}_8^{(n-1)}}{\alpha_1^{(n-1)}(\omega) + W^{(n-1)}}$$

(see e.g. system (3.3)), and since

$$\tilde{P}_8^{(n-1)}(\omega) = \frac{\alpha_1^{(n-1)}(\omega) + W^{(n-1)}}{(\alpha_1^{(n-1)}(\omega) + W^{(n-1)})(\alpha_3^{(n-1)}(\omega) + 2 + W^{(n-1)}) - W^{(n-1)}} \tilde{P}_4^{(n-1)} = \tilde{P}_2^{(n)} \quad ,$$

we have

$$\tilde{P}_9(\omega) = \prod_{k=0}^{n-2} \left[\frac{(\alpha_1^{(k)}(\omega) + W^{(k)})(\alpha_3^{(k)}(\omega) + 2 + W^{(k)}) - W^{(k)}}{\alpha_1^{(k)}(\omega) + W^{(k)}} \right] \frac{\alpha_1^{(n)}(\omega) + W^{(n)}}{\left(\alpha_1^{(n-1)}(\omega) + W^{(n-1)}\right) \Delta^{(n)}} \quad . \tag{4.4}$$

Applying the above outlined asymptotic analysis to $\tilde{P}_9$, one finally arrives to

$$P_9(t) \approx \frac{\left(1 - W^{2^{n-1}}\right)}{1 - W^2} \frac{W^{2^{n-1}}}{2\ 2^n} e^{-t/t_n^*} \quad ; \tag{4.5}$$

notice the $W^{2^{n-1}}$ extra factor, comparing to eq.(4.3c). In a similar way we calculate occupation probabilities of another tip site, number 3, which is closer to the bias origin, and another site with coordination 3, number 8,

$$P_3(t) \approx \frac{\left(1 - W^{2^{n-1}}\right)}{1 - W^2} \frac{3W^{2^n}}{16\ 2^n} e^{-t/t_n^*} \quad , \tag{4.6a}$$

$$P_8(t) \approx \frac{\left(1 - W^{2^{n-1}}\right)}{1 - W^2} \frac{W^{2^n}}{4\ 2^n} e^{-t/t_n^*} \quad . \tag{4.6b}$$

The above results, (4.3,5,6), again point out how in a branch of linear size L, all occupation probabilities, as well as the FPP, decay with the same characteristic time $t^* \sim e^{|\ln W| L/2}$. In an infinite structure with branches of any length scale, the larger is the branch, the exponentially longer will be the time the particle spends in it, due to trapping effects caused by the bias. This will cause a logarithmic slowing down of diffusion.

Strong evidence that the bias drives the particle into the deepest dangling ends can also be drawn by looking at the amplitude dependence of occupation probabilities. Indeed we notice that the $P(t)$ of tip sites which are at maximum chemical distance from the bias source, have an amplitude factor proportional to $1/2^n$ (see eq.(4.3c); an identical result holds for site 6). The number of such sites grows just as 2^n with the order n of the T fractal, because the branch containing the absorbing site has not to be taken into account due to its depleting nature (compare for example eq.(4.3c) with (4.3d) and (4.5)). Hence we infer that, after a transient time, probability accumulates into these deep dangling ends, redistributing then slowly against the biasing force to sites with higher coordination and/or in less favourable positions. Amplitude factors for the probability of every other kind of site are in fact proportional to $W^\eta/2^n$, where the exponent η depends manifestly, though non trivially, on the chemical distance between the site under consideration and those deepest dangling end, namely on the number of unfavourably biased bonds one has to cross going from the latter to the former. In an infinite size limit, occupation probabilities of sites with coordination > 1 will then be vanishingly small compared with those relative to the dangling ends,

in agreement with our hypothesis.

Finally we would like to point out the peculiar features of the sink site. This site can not be considered, like other tips, as a probability accumulating point, of course, and the same applies to its neighbouring sites (e.g. number 9 in Fig.2.1b). Such circumstance reflects on the W^{2^n} and $W^{2^{n-1}}$ prefactors in eqs.(4.3d) and (4.5), respectively. Moreover $\tilde{P}_{10}$ (i.e. $\tilde{P}_{FP}$) has actually two simple poles: $\omega_{c1} = -\frac{1}{W_+}$ and $\omega_{c2} \overset{n\to+\infty}{\cong} -1/W_+ t_n^*$, as it appears from eqs.(3.6,12). Therefore two characteristic times exist, the first deriving from ω_{c1}, very short and connected to the transient time when the initial flux of probability entering the side branch is immediately absorbed by the sink. The second, t_n^*, is quite long and corresponds to the asymptotic regime when probability formerly accumulated into deep dangling ends slowly reflows in the whole lattice and then is absorbed by the sink.

To probe a possible dependence of diffusion process on initial conditions, we have studied the same model choosing different input sites, namely no longer site 1, but either 4 or 7 of Fig.2.1b, successively. We arrived at exactly the same results for $\langle t \rangle^{(n)}$, t_n^*, $P_{FP}(t)$ and occupation probabilities. Hence we claim that the above results and considerations hold for our model independently of initial conditions.

The description of the dynamic model we are concerned with, should be independent on the particular realization of the bias pattern. To get convinced of this, a less asymmetric situation than that presented in Fig.2.1, has also been considered. Again, starting from a T fractal, we suppose to orient the arrows of topological bias as in Fig.4.1. This new choice, together with the conventions on W_{ij} specified in section 2 [21], implies that the bias pushes a diffusing particle away from the T fractal central site (number 2 in Fig.4.1a, or 4 in Fig.4.1b). In addition the three tip-sites (e.g. 1,7,10 in the 2-order lattice of Fig.4.1b) are assumed to be absorbing, and the central one to be the input point of the walker. Master equations and their Laplace transforms are equivalent to (2.1) and (2.4) respectively, with the difference that now $\alpha_0(\omega)$ refers to the central site, which has three nn, but is not dynamically equivalent to other 3-coordinated sites. The method outlined in section 3 and the present one applies of course to the latter model too. Considering an nth-order tree one finds, for relevant quantities:

$$\langle t \rangle^{(n)} \propto \frac{L}{2W^{L/2}} \tag{4.7a}$$

$$t_n^* \simeq \frac{(1+W)}{W_+} \frac{2^n}{W^{2^{n-1}}} \tag{4.7b}$$

$$P_{1,7,10}(t) \approx \frac{W^{2^{n-1}}}{3\ 2^{n-1} + 3W_+ W^{2^{n-1}}} e^{-t/t_n^*} \tag{4.7c}$$

$$P_4(t) \approx \frac{(1-W^{2^n})}{1-W^2} \frac{W^{2^n}}{3\ 2^n} e^{-1/t_n^*} \tag{4.7d}$$

$$P_{3,6,9}(t) \approx \frac{(1-W^{2^{n-1}})}{1-W^2} \frac{1}{3\ 2^n} e^{-t/t_n^*} \tag{4.7e}$$

$$P_{2,5,9}(t) \approx \frac{(1-W^{2^{n-1}})}{1-W^2}\frac{2W^{2^{n-1}}}{3\ 2^n}e^{-t/t_n^*} \quad . \tag{4.7f}$$

Site indices, shown in Fig.4.1b, are those which would apply after $n-1$ decimations. Taking into account that the linear size of the nth-order lattice is 2^{n+1}, but that each of its three branches is indeed equivalent to the $(n-1)-$order lattice of Fig.2.1, and its length is thus $L = 2^n$, then results (4.7) are totally consistent with previous ones. This is not surprising in view of the threefold symmetry implied by the conditions we imposed.

So, our analysis applies to different realizations of the present model. It can also be shown that our approach can be extended to a wider family of ramified fractals, like for example that in Fig.2.2, in $d \geq 2$ dimensions.

5 Conclusions

We have considered the problem of random walks on deterministic self-similar trees in the presence of a topological biasing field. Relying on FSS ideas, we have developed a method to extract the FSS behaviour of the average FPT, $\langle t \rangle$, and characteristic time, t^*. The method is phenomenological and is based on successive decimations and rescalings of the set of master equations for a finite nth-order lattice. $\langle t \rangle$ and t^* are found to scale in the same way with the system size, L, i.e. $\langle t \rangle \sim t^* \sim \frac{L}{W^{L/2}}$. Thus, dynamics is controlled by a unique time scale growing exponentially with the tree's size. Since infinite fractal trees contain branches of any length scale, where the particle can be trapped in, we argue that the resulting slowing down should indeed lead to the logarithmic diffusion conjectured for infinite systems. Moreover, the existence of a unique time scale reveals a substantial equivalence between the fixed time and the fixed point of observation ensembles, governing the behaviour of $\langle R(t) \rangle$ and $\langle t \rangle$, respectively. The scaling of t^* implies also a divergence of the dynamical exponent z and thus a singularity in standard RG transformations for infinite lattice. The possibility to carry on a phenomenological RG strategy in the presence of singular transformations, via the expedient of considering systems of finite size, should be seen as the main achievement of our technique, in view of the serious complications involved in the RG analysis of infinite systems [12]. It is also worth noting that we produced here an interesting example of the validity of the FSS hypothesis, notwithstanding the existence of a singularity in the RG group.

Finite size analysis has been pushed further here to calculate the long time behaviours of FPP and occupation probabilities, by combining asymptotic expansion of the respective Laplace transforms with RG rescalings. All probabilities are found to decay exponentially at long t , again with the same characteristic time t^*, as expected. This fact, of course, supplies stronger confidence to the picture of logarithmic diffusion generated by the mechanism of bias induced trapping into dangling ends. Amplitude factors of occupation probabilities offer further insight into this dynamic process. Indeed, the occupation probabilities of sites located in the deepest dangling ends have amplitude proportional to $1/2^n$, which is just

the inverse of their number in an nth order lattice. Moreover, probabilities relative to sites with higher coordination or in a less favourable position with respect to the biasing field, have amplitudes proportional to $W^{\eta}/2^{n}$ $(W < 1)$, with η depending on the chemical distance between the deepest dangling ends and the site under consideration. Thus probability first accumulates into the longest branches of the fractal under the bias drift; then it very slowly reflows against the bias to the whole lattice, generating the logarithmic slowing down of diffusion.

The above results have been demonstrated to hold in general for the system under discussion, no matter which initial and boundary conditions are chosen, and independently of the particular realization of the model. Our methods can be applied to a wide variety of finitely ramified fractals [18], for which they provide the same picture of logarithmic biased diffusion outlined here.

Acknowledgments

We are indebted to A. Maritan for collaboration in the early stages of our work on logarithmic diffusion.

References

[1] E. Marinari, G. Parisi, D. Ruelle and P. Widney, *Phys. Rev. Lett.* **50**, 1223 (1983).

[2] D.S. Fischer, *Phys. Rev. A* **30**, 960 (1984); D.S. Fisher, D. Friedan, Z. Qiu, S.J. Shenker and S.H. Shenker, *Phys. Rev. A* **31**, 3841 (1985).

[3] R. Durrett, *Commun. Math. Phys.* **104**, 87 (1986).

[4] R.L. Bulmberg Selinger, S. Havlin, F. Leyvraz, M. Schwartz and H.E. Stanley, *Phys. Rev. A* **40**, 6755 (1989).

[5] M. Nauenberg, *J. Stat. Phys.* **41**, 803 (1985).

[6] A. Bunde, S. Havlin, H.E. Roman, G. Schildt and H.E. Stanley, *J. Stat. Phys.* **50**, 1271 (1988).

[7] Ya.G. Sinai, *Theory Prob. its Appl.* **27**, 256 (1982).

[8] D. Stauffer, *J. Phys. A* **18**, 1827 (1985).

[9] A. Bunde, H. Harder, S. Havlin and H.E. Roman, *J. Phys. A* **20**, L865 (1987).

[10] S. Havlin, A. Bunde, Y. Glaser and H.E. Stanley, *Phys. Rev. A* **34**, 3492 (1986).

[11] Sinai's and related results [1,3-7] are intuitively explained once it is realized that over a distance R along the 1D chain, a potential barrier $\propto \sqrt{R}$ develops by adding local random biases with zero average. On the basis of Arrhenius law, a time $t \propto e^{\sqrt{R}}$ is needed to overcome such a barrier, then $R \sim \ln^2 t$ follows.

[12] A. Maritan, G. Sartoni and A.L. Stella, *Phys. Rev. Lett.* **71**, 1027 (1993).

[13] S. Havlin and D. ben-Avraham, *Adv. Phys.* **35**, 695 (1987).

[14] A. Giacometti, A. Maritan and A.L. Stella, *Int. J. Mod. Phys. B* **5**, 709 (1991).

[15] R. Stinchcombe, *J. Phys. A* **18**, L591 (1985).

[16] M. Suzuki, *Prog. Theor. Phys.* **58**, 1142 (1977).

[17] B. Kahng and S. Redner, *J. Phys. A* **22**, 887 (1989).

[18] This is the most simple example in $d = 2$ of a whole class of ramified fractals in d dimensions, which can all be treated with our methods (see Fig.2.2).

[19] A. Giacometti, A. Maritan and A.L. Stella, *Phys. Rev. B* **38**, 2758 (1988).

[20] It is important that $\omega_c \overset{n\to+\infty}{\longrightarrow} 0$, because we look at the asymptotic behaviour, $\omega \to 0$, of $\tilde{P}_{FP}$. Were the simple pole located elsewhere, we could not find it by the asymptotic analysis.

[21] Actually the condition $3W_+ \leq 1$ has to be added to what stated in section 2, to take into account the peculiar nature of the central site.

FIGURES

FIGURE 2.1 The first three successive iterations of the T fractal, (a), (b) and (c) respectively. The arrows on each bond indicate the direction of the topological bias.

FIGURE 2.2 Example of T fractal with coordination 4 or 1, in $d = 2$. Analogous lattices can be drawn in $d > 2$.

FIGURE 4.1 The first two iterations of the symmetric T fractal lattice, (a) and (b) respectively, with a topological bias on each bond.

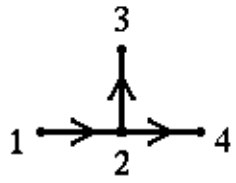

(a)

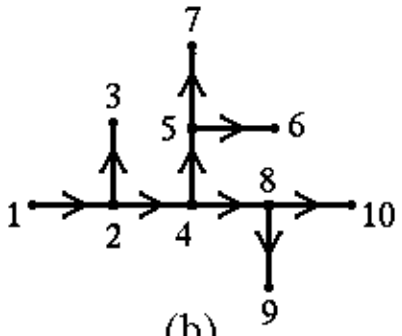

(b)

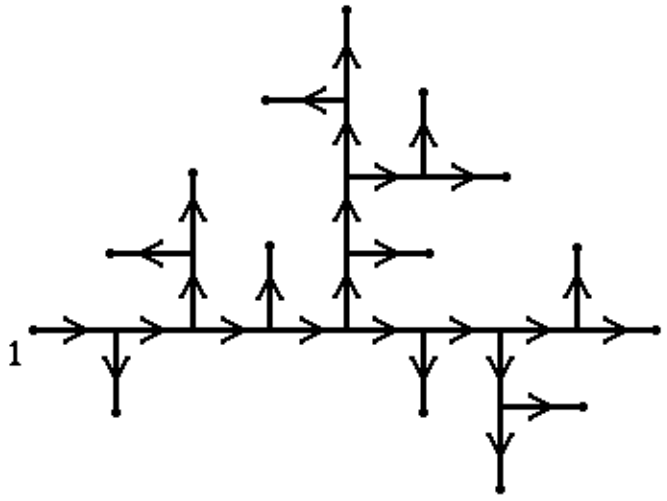

(c)

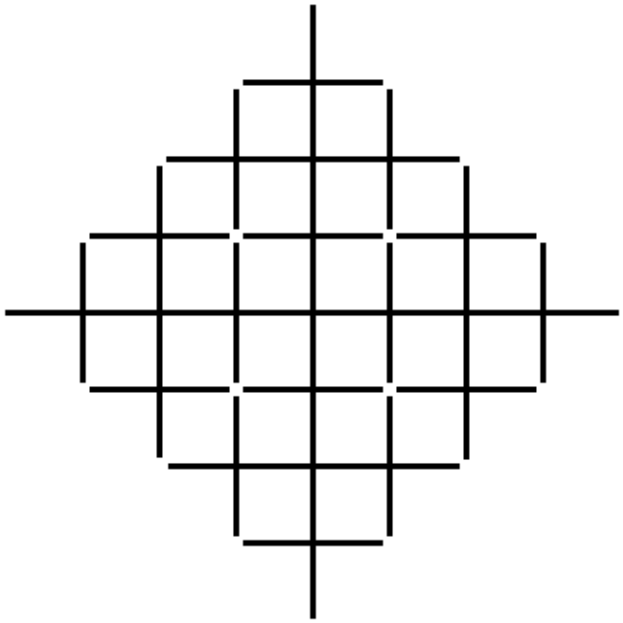

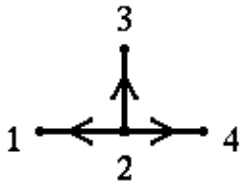

(a)

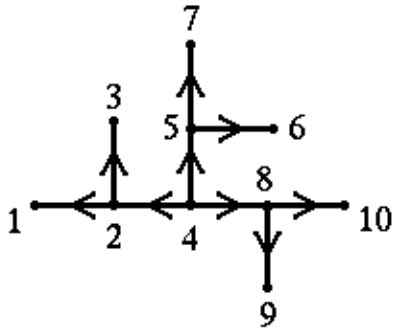

(b)